



## Adhesion Performance and UV-Curing Behaviors of Interpenetrated Structured Pressure Sensitive Adhesives with 3-MPTS for Si-Wafer Dicing Process

Seung-Woo Lee , Ji-Won Park , Yong-Hee Lee , Hyun-Joong Kim , Miriam Rafailovich & Jonathon Sokolov

To cite this article: Seung-Woo Lee , Ji-Won Park , Yong-Hee Lee , Hyun-Joong Kim , Miriam Rafailovich & Jonathon Sokolov (2012) Adhesion Performance and UV-Curing Behaviors of Interpenetrated Structured Pressure Sensitive Adhesives with 3-MPTS for Si-Wafer Dicing Process, Journal of Adhesion Science and Technology, 26:10-11, 1629-1643

To link to this article: <https://doi.org/10.1163/156856111X618452>



Published online: 24 Jul 2012.



Submit your article to this journal [↗](#)



Article views: 91

# Adhesion Performance and UV-Curing Behaviors of Interpenetrated Structured Pressure Sensitive Adhesives with 3-MPTS for Si-Wafer Dicing Process

Seung-Woo Lee<sup>a</sup>, Ji-Won Park<sup>a</sup>, Yong-Hee Lee<sup>a</sup>, Hyun-Joong Kim<sup>a,b,\*</sup>,  
Miriam Rafailovich<sup>b</sup> and Jonathon Sokolov<sup>b</sup>

<sup>a</sup> Laboratory of Adhesion & Bio-Composites, Program in Environmental Materials Science, Research Institute for Agriculture & Life Science, Seoul National University, Seoul 151-921, Republic of Korea

<sup>b</sup> Department of Materials Science and Engineering, State University of New York at Stony Brook, NY11794, USA

Received on 15 April 2011; revised 21 June 2011; accepted 21 June 2011

## Abstract

As Si-wafers, as used in the electronic industry, become thinner and thinner, it is important to investigate the conditions which are suitable for easily peelable acrylic dicing tapes. In the 'pick-up' process, the adhesion strength decreased after UV irradiation as a result of polymer network formation. In this study, interpenetrating polymer network (IPN) structured acrylic pressure sensitive adhesives (PSAs) were investigated with two different types of UV irradiation — a steady UV irradiation and a pulsed UV irradiation of 100 mJ/cm<sup>2</sup>. The PSAs binder contained 2-ethylhexyl acrylate (2-EHA), acrylic acid (AA) and 3-methacryloxypropyl trimethoxysilane (3-MPTS). The hexafunctional monomer, dipentaerythritol hexacrylate (DPHA) and 3-methacryloxypropyl trimethoxysilane (3-MPTS) were used as diluent monomers. The adhesion performance as related to the peel strength and the tack properties on the Si-wafer substrates, was examined with increasing UV dose. The effect of UV-curing on the behavior and viscoelastic properties of the 'pick-up' acrylic tapes was investigated using Fourier transform infrared — attenuated total reflectance spectroscopy (FTIR-ATR) and an advanced rheometric expansion system (ARES). It is also necessary to consider the contaminants on the Si-wafer substrates left behind after releasing the dicing tapes, because of possible damage to the Si-wafers and subsequent processes. Field emission scanning electron microscopy (FE-SEM) and X-ray photoelectron spectroscopy (XPS) analysis revealed little residue on the Si-wafer after removing the tapes and after more than the specific level of UV dose.

© Koninklijke Brill NV, Leiden, 2012

\* To whom correspondence should be addressed. E-mail: hjokim@snu.ac.kr

**Keywords**

Pressure sensitive adhesives, Si-wafer, UV irradiation, dicing tapes, interpenetrating polymer networks (IPN)

**1. Introduction**

A pressure sensitive adhesive (PSAs) is a type of adhesive that can be attach to a substrate using only a low pressure contact — it does not require any reaction process as do other types of adhesives [1]. PSAs are being used in various products such as adhesive tape, labels, protective and decorative foils [2]. Their functional characteristics such as instantaneous adhesiveness, repeated adhesiveness, tackiness, etc. as well as their ease of application make them a popular choice in many applications. Together with the expanding applications for PSA, their capabilities are also widening as a result of new types of PSA being developed [3].

Increasing market demand has driven the semiconductor industry to miniaturize all the materials used in semiconductor packaging. The adhesives that bond integrated circuit (IC) chips to substrates have also followed the market trend towards miniaturization. Film adhesives are able to satisfy this demand, and are now widely used, having replaced conventional liquid adhesives [4]. Film adhesives are generally provided as an adhesive tape composed of an adhesive layer and a base material. The tape is laminated on a wafer during the semiconductor manufacturing process. The wafer is then divided into IC chips using a rotary blade. The IC chip and the attached film adhesive are peeled away from the base material using protruding needles in a process called ‘pick-up’ [5, 6].

An excessive degree of cross-linking in PSAs prepared from unsaturated polyester resins by electron beam irradiation, results in poor adhesive strength [7, 8]. This observation led us to establish a dicing process, as shown in Fig. 1. A piece

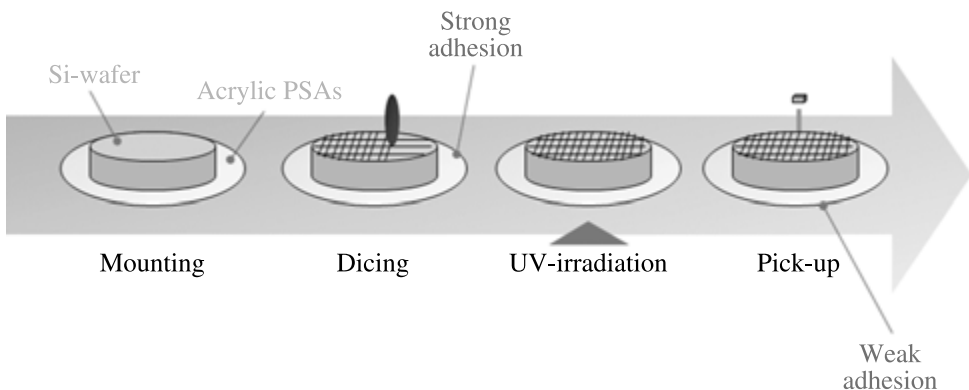


**Figure 1.** Schematic diagram of the dicing process on thin Si-wafer manufacture applied with acrylic PSAs.

of silicon wafer was tightly held using a dicing tape with strong adhesion strength, which enables rapid and smooth dicing of the wafer. Subsequently, the adhesive layer was irradiated with UV light through the reverse side of the substrate. After UV irradiation, the adhesion strength decreased to a certain level, making it easy to pick up the diced chips for further die-bonding processes. Dicing tapes developed using this process have been reported [7, 9, 10] and similar suggestions have been made [7, 11, 12].

Acrylic monomers and oligomers are used widely on account of their superior properties of transparency, colorlessness, resistance to yellowing under sunlight and resistance to oxidation due to their saturated structures. However, they have poor thermo-mechanical stability because of their linear structure. Therefore, cross-linking of multifunctional acrylates is needed to increase their thermo-mechanical stability. Kaczmarek and Decker [13, 14] reported that an adhesive shows fluid-like behavior when it is widely cross-linked. However, the more cross-linked is the adhesive, the greater is the creep resistance [13, 15]. Multifunctional acrylates cross-link rapidly by radical and cationic polymerization; the kinetics and properties of these polymers have been investigated [13, 16]. Cross-linked acrylates produce interpenetrating polymer networks (IPNs). These IPNs are a combination of two cross-linked polymers (each made *via* independent reaction processes) held together by permanent entanglements and are prepared using special methods [17]. The absence of cross-reactions between the two networks is an important condition to ensure morphology control [18–21].

In this study, the IPN structured acrylic PSAs used in the Si-wafer ‘pick-up’ process were prepared using a dipentaerythritol hexacrylate, 3-methacryloxypropyl trimethoxysilane with a UV-curing system using two different types of UV irradiations. Emphasis was placed on the conditions required for easy of peeling. The effect of the UV-curing on the behavior, viscoelastic properties and molecular distribution were investigated using Fourier transform infrared (FTIR), gel permeation chromatography (GPC) and an advanced rheometric expansion system (ARES). Finally, field emission scanning electron microscopy (FESEM) and X-ray photoelectron spectroscopy (XPS) revealed little residue on the wafer on releasing the film after UV irradiation.

## 2. Experimental

### 2.1. Materials

The compounds 2-ethylhexyl acrylate (2-EHA, 99.0% purity, Samchun Pure Chemical Co., Ltd, Republic of Korea) and acrylic acid (AA, 99.0% purity, Samchun Pure Chemical Co., Ltd, Republic of Korea) were commercially available and used without purification. Ethyl acetate (EAc, Samchun Pure Chemical Co., Ltd, Republic of Korea) and methanol (MeOH, Samchun Pure Chemical Co., Ltd, Republic of Korea) were used as solvents and 2,2'-azobisisobutyronitrile (AIBN, Junsei Chemical, Japan) was used as a thermal initiator. Methylaziridine derivative (MAZ, DSM

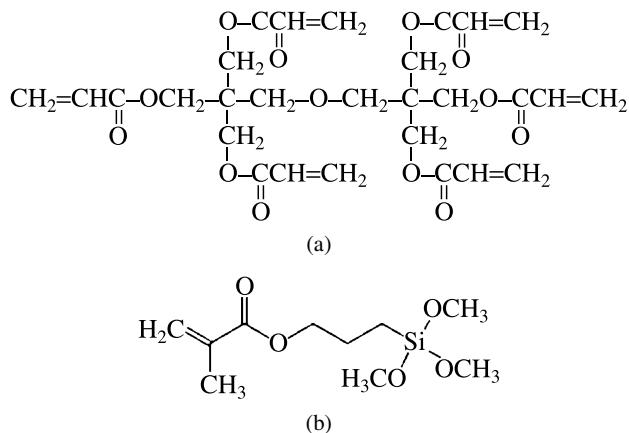


**Figure 2.** Chemical structure of the dipentaerythritol hexacrylate (DPHA) (a) and 3-methacryloxypropyl trimethoxysilane (3-MPTS) (b).

Neoresins, USA) was used as the cross-linking agent. Dipentaerythritol hexacrylate (DPHA, Miwon Specialty Chemical, Republic of Korea) and 3-methacryloxypropyl trimethoxysilane (3-MPTS, Dow Corning Toray Co., Ltd, USA) were used as the diluent monomer. Figure 2 shows the chemical structure of hexafunctional acrylate which has six C=C double bonds and silicone-modified acrylate. The compound 2-Hydroxy-2-methyl-1-phenyl-propane-1-one (Miwon Specialty Chemical, Republic of Korea) was used as the photo-initiator.

## 2.2. Methods

### 2.2.1. Synthesis of Binders

Acrylic monomers (2-EHA, AA, 3-MTPS) were synthesized as 95, 4.5 and 0.5 wt% by solution polymerization. The amount of AIBN in the binders was 0.3 phr and the solid content was 40%. The mixture was placed into a 500 ml four-neck flask equipped with a stirrer, condenser and thermometer, and heated to 75°C with constant stirring. At the end of the exothermic reaction, the temperature was maintained for 30 min, and a blend of ethyl acetate and AIBN was added. The reaction was allowed to proceed for 0.5 and 2.5 h. Finally, polymerization was terminated by cooling the mixture to room temperature. The prepared pre-polymers were used as PSAs [22].

### 2.2.2. Formation of PSA Films

All the acrylic PSAs were coated onto the corona treated polyethylene terephthalate (PET, SK Chemical, Republic of Korea) film using coating bars, kept at room temperature for 1 h and then dried in an oven at 80°C for 20 min. These dried films were kept at 22 ± 2°C and 60 ± 5% RH for 24 h before used in the experiments [23].

### 2.2.3. Preparation of Cured Acrylic PSAs

Acrylic PSAs were cured with the addition of a curing agent followed by UV-curing. The curing agent was a multifunctional methylaziridine. The cross-linking

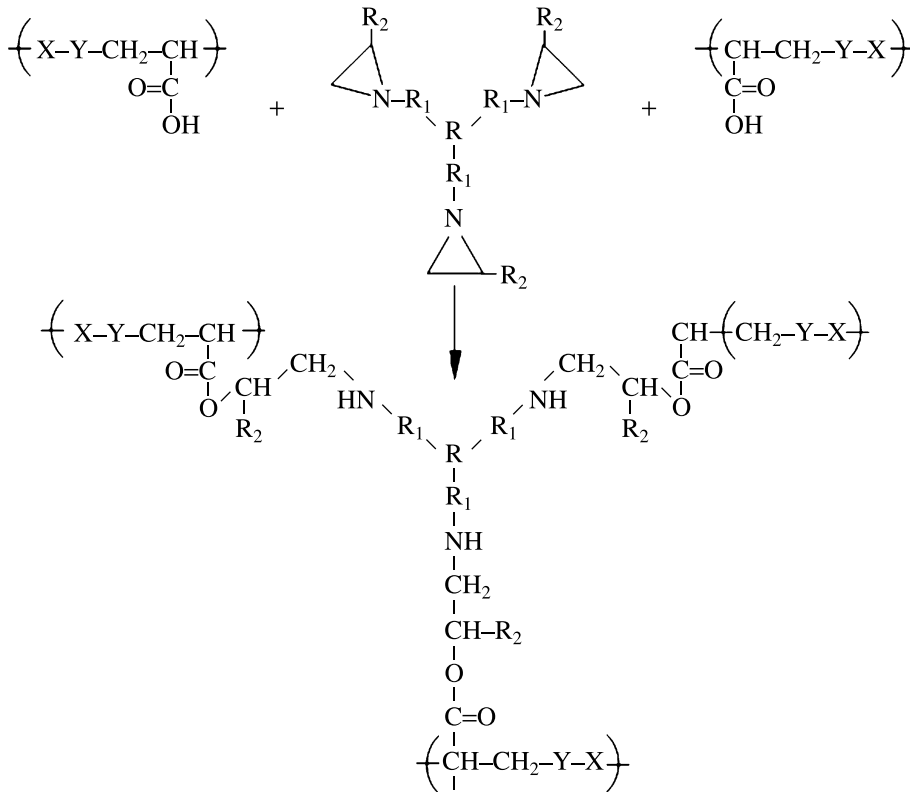


**Figure 3.** Cross-linking of carboxylated PSA with methylaziridine [24].

of the PSAs with the multifunctional methylaziridine involves mainly the carboxyl groups of the vinyl carbonic acids within the polymeric chain. The oxygen of the nucleophilic carboxyl group causes ring opening of the aziridine rings, whereas the hydrogen atoms of the carboxyl groups protonate the nitrogen atoms (Fig. 3) [24]. The UV-curable PSAs were prepared by blending polymerized binders with a photo-initiator and a hexafunctional acrylic monomer. The UV-curable PSAs were coated onto polyethylene terephthalate (PET or polyester) films and cured using conveyor belt type UV-curing equipment with a 100 J/s high pressure mercury lamp (main wavelength: 365 nm). The UV doses were measured using an IL 390C Light Bug UV radiometer (International Light, USA). Despite low molecular weights, the hexafunctional monomers in the PSAs can be photo-polymerized after a UV dose to form the IPN structures (Fig. 4) [22].

#### 2.2.4. Adhesion Performance

The prepared acrylic PSAs films were attached to a silicon wafer substrate and a 2 kg rubber roller was passed over them twice. The 180° peel strength was measured using a Texture Analyzer (TA-XT2i, Micro Stable Systems, UK) after the sample was left to stand at room temperature for 24 h. The peeling speed was 300 mm/min,

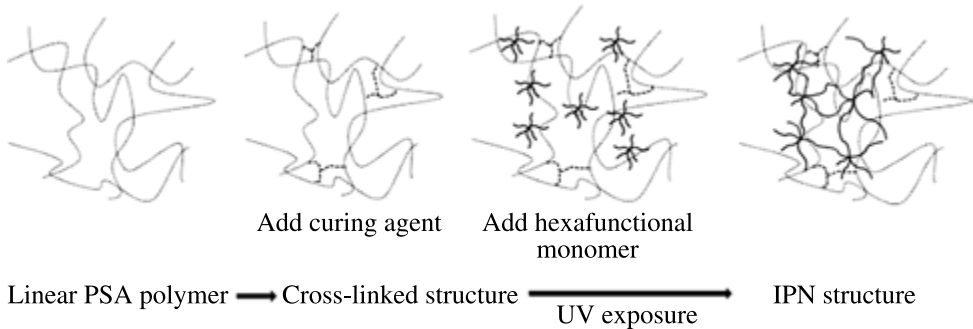


**Figure 4.** Process of producing IPN structures in UV-cured dicing acrylic PSAs [22].

and the average strength of peeling period was measured five times. The probe tack was measured with a 5 mm diameter stainless steel cylindrical probe using the Texture Analyzer. The approaching speed of the probe was 0.5 mm/s and was in contact with the surface of PSAs for 1 s at a constant pressure of 100 g/cm<sup>2</sup>. The debonding speed was 0.5 mm/s and the probe tack was measured as the maximum debonding force (ASTM D3330) [22].

#### 2.2.5. Fourier Transform Infrared (FTIR) Spectroscopy

The FTIR spectra were obtained using an FTIR-6100 (JASCO, Japan) installed with an attenuated total reference (ATR) accessory composed of a zinc selenium (ZnSe) crystal with a 45° angle of incidence. The spectra were recorded for 30 scans with a 4 cm<sup>-1</sup> resolution over the wavelength range 650–4000 cm<sup>-1</sup>. The curing behavior of the acrylic PSAs samples were characterized by monitoring the changes in the C=C bond and carboxylic group at 810 cm<sup>-1</sup> and at 1730 cm<sup>-1</sup>. All the results were confirmed by determining the level of CO<sub>2</sub> reduction, H<sub>2</sub>O reduction, noise elimination, smoothing and baseline correction. The curing behavior of cross-linking with the UV dose was obtained using the FTIR–ATR.

#### 2.2.6. Gel Permeation Chromatography (GPC) Measurement

The samples were eluted using tetrahydrofuran (THF) at room temperature and filtered through a 0.2 μm polytetrafluoroethylene (PTFE) syringe filter. Molecular weights were measured by GPC at 35°C using a YL-CLARITY system (Young-Lin Instrument Co., Ltd) equipped with a refractive index (RI) detector and a Polymer Labs PL-gel 10 μm column (two mixed-B). THF was used as an eluent solvent at a flow rate of 1 ml/min. The number-average ( $M_n$ ) and weight-average ( $M_w$ ) molecular weights were calculated using a calibration curve from polystyrene standards.

#### 2.2.7. Advanced Rheometric Expansion System (ARES) Analysis

The viscoelastic properties of the acrylic PSAs were determined using an advanced rheometric expansion system (ARES, Rheometric Scientific, UK, in NICEM at Seoul National University) equipped with an 8 mm parallel plate mode. The typical temperature scan range was 60–200°C, and the heating rate was 5°C/min. The fre-

quency was 1 Hz and the gap between the plates was 1 mm. Also the  $\tan \delta$  curves from the temperature sweep tests suggests a glass transition temperature ( $T_g$ ).

#### 2.2.8. Field-Emission Scanning Electron Microscopy Observation

The morphology of each sample after the peel strength test was measured by field-emission scanning electron microscopy (FE-SEM) (SUPRA 55VP, NICEM at Seoul National University). The fractured samples were coated with a thin layer of gold (purity 99.99%) prior to the FE-SEM examination to prevent electron charging [25].

#### 2.2.9. X-Ray Photoelectron Spectroscopy (XPS) Analysis

X-ray photoelectron spectroscopy (XPS, PHI 5000 Versa Probe, Ulvac-PHI) was performed using  $AlK_{\alpha}$  radiation (1486.6 eV, anode (25 W, 15 kV)). The binding energies were calibrated with reference to the  $C_{1s}$  peak at 284.6 eV. For the measurement, the samples were placed into an ultra high vacuum chamber. Data analysis of the sensitivity factors of each element present was performed [26–28].

### 3. Results and Discussion

#### 3.1. Adhesion Performance

The most important factors of the UV cross-linked acrylic PSAs, peel strength and tack properties, can be handled by the UV dose. In a production plant the UV dose can be controlled by adjusting the power of the lamps and/or the speed at which the Si substrate is passed under lamps. The solvent borne UV-cross-linkable acrylic PSA is coated directly and after removing the solvents the adhesive film is cross-linked by UV-irradiation and in a transfer process, depending on the carrier material, to produce the adhesive properties as required [29]. In this study, one of our aims was to examine the influence of the UV dose on the  $180^\circ$  peel strength and tack property of the PSA samples using two types of irradiation systems. These were the steady irradiation and the pulsed irradiation of  $100 \text{ mJ/cm}^2$ . The results of the trials are presented in Figs 5 and 6. Cohesive failure, which means that there was little residue, was only observed on the initial peel strength and tack property test which did not involve a UV dose. The interfacial failures showed that there was no residue on the other samples. With the increase of UV dose, the peel strength and the tack property of the PSAs decreased slightly. This was still at an acceptable level because the peel strength is the sum of the energies required to break the bond and deform the backing and the PSA [30]. UV-cross-linking promotes the modulus property of the PSA, and as a result the elongation of PSA was reduced after UV curing. The reason why the tack property for PSAs specimens decreases after UV irradiation is attributed to the fact that the cross-link increased the stiffness of PSAs [26]. Similar results have been reported in the literature [31]. The peel strength and the tack property of the pulsed UV irradiation (at  $100 \text{ mJ/cm}^2$ ) were lower than those of the steady irradiation as shown Figs 5 and 6. That is, the pulsed irradiation (at  $100 \text{ mJ/cm}^2$ ) indicates poorer adhesion strength which is



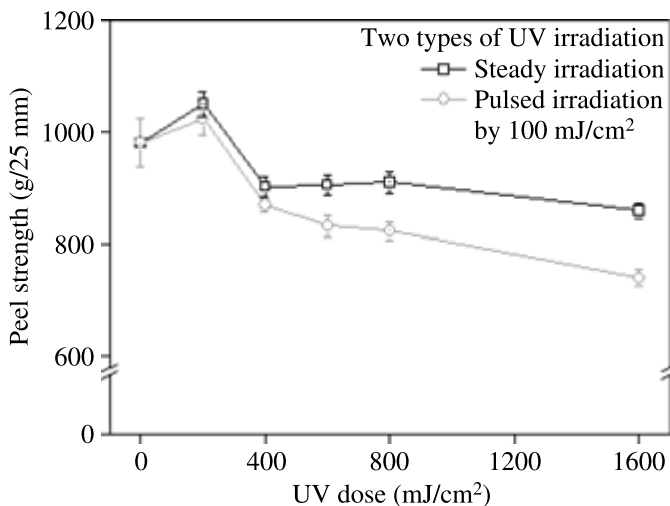


**Figure 5.** Peel strength of PSAs by two types of UV irradiation.

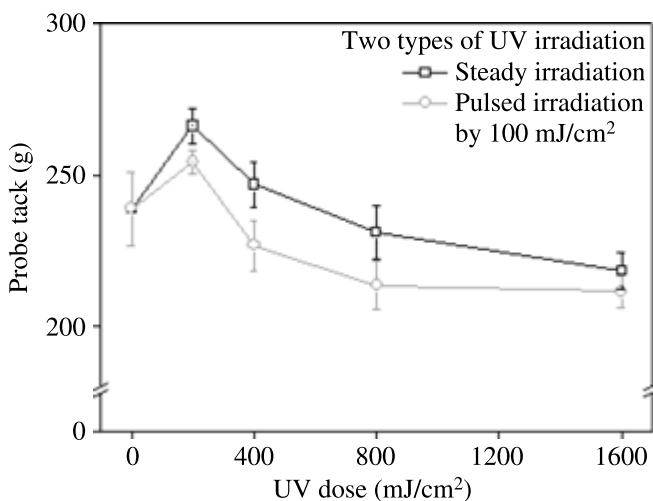
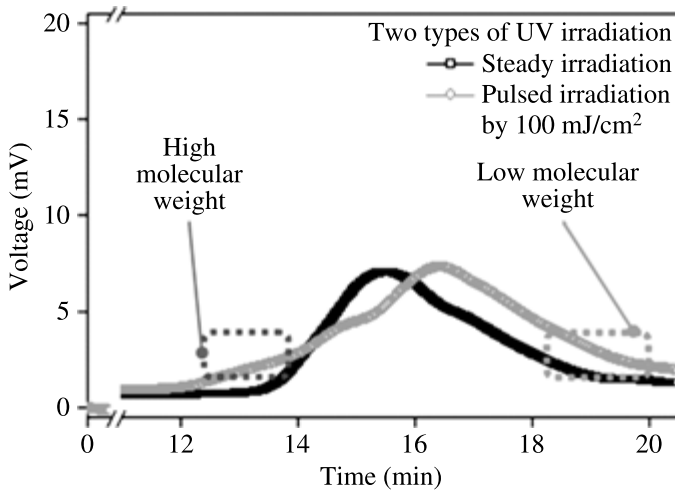


**Figure 6.** Probe tack of PSAs by two types of UV irradiation.

attributed to inhomogeneous cross-linked network structures. This was confirmed by the GPC measurements as shown Fig. 7. A higher PDI (polydispersity index) was produced using the pulsed irradiation at  $100 \text{ mJ/cm}^2$ . As can be seen in Fig. 7, both the higher and lower molecular weight areas appear remarkable after pulsed irradiation at  $100 \text{ mJ/cm}^2$ . Results from this study, thus, show that the pulsed UV-irradiation method is successful and efficient.

### 3.2. Viscoelastic Properties

The viscoelastic properties are important in the adhesion performance of acrylic PSAs. In this work the effect of the different UV doses were tested using ARES



	$M_w$ (g/mol)	$M_n$ (g/mol)	PDI ( $M_w/M_n$ )
Steady	201 000	33 000	5.9
Pulsed	267 000	16 000	16.1

**Figure 7.** GPC measurement of PSAs by two types of UV irradiation.

measurements. The storage modulus ( $G'$ ) is linked with the hardness of the adhesive, and the loss modulus ( $G''$ ) is related to energy absorption. The values indicate the balance of the viscoelastic behavior. After UV irradiation, the adhesive strength of a PSA composition including DPHA and 3-MTPS decreased drastically compared with other compositions. Because of the network formation due to the UV irradiation, this composition had a greater volume contraction. This could lead to micro-voids at the interface between the adhesive and the silicon wafer, resulting in a loss of adhesion [7]. A higher storage modulus was expected to be more suitable for supporting the silicon wafer during the dicing and picking up of the diced chips, together with the adhesive layer from the face material [8]. Figure 8 shows that the storage modulus of acrylic PSAs are different, particularly at high temperatures. The storage modulus of the acrylic PSAs with UV dose was higher than the acrylic PSA without UV dose over about 25°C. It can be showed that PSA's cohesion gets higher with increasing UV dose. Furthermore, the plateau area of the storage modulus in the high temperature region indicates that acrylic PSAs formed an entanglement structure. As shown in Fig. 8, the storage modulus at high temperatures is directly related to the thermal resistance of acrylic PSA. Therefore, acrylic PSAs become more elastic at high temperatures with increasing UV dose. Figure 9 shows the  $\tan \delta$  curve of acrylic PSA as a function of the UV dose. The  $T_g$  of the trials (temperature at  $\tan \delta$  peak) was similar. Moreover, the  $\tan \delta$  of the acrylic PSAs decreased with increasing UV dose. This suggests that the storage

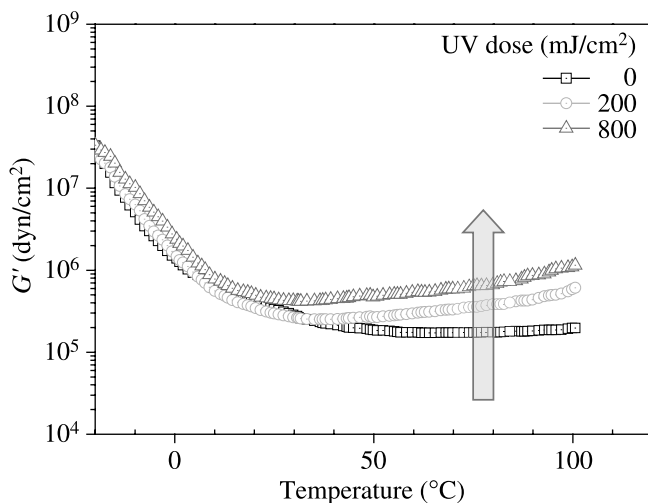


**Figure 8.** Temperature dependence of storage modulus  $G'$  with different UV dose.

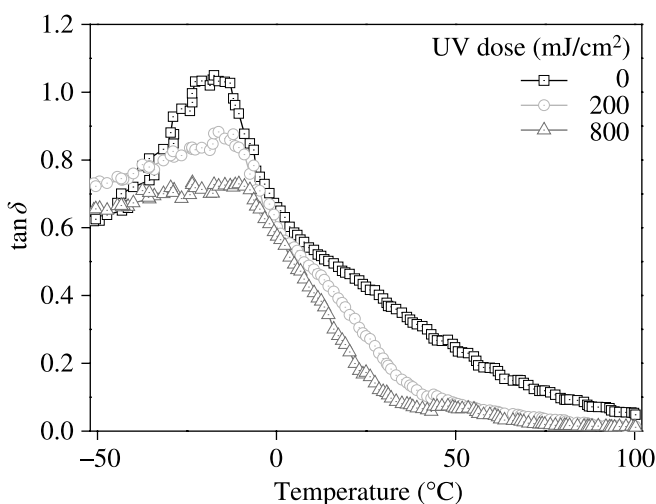


**Figure 9.** Tangent delta of UV-cured acrylic PSAs.

modulus of the acrylic PSAs is strongly associated with the UV dose in the room temperature region. Hence,  $\tan \delta$  also decreased with increasing UV dose.

### 3.3. FTIR–ATR Spectroscopy

The kinetics of the photo-induced cross-linking was investigated using FTIR–ATR. After photo-initiation by UV dose at a certain wavelength, multi-functional monomers proceeded to polymerize. These monomers formed a cross-linked IPN structure. The curing behavior of functional monomers can be monitored using FTIR because the C=C twisting vibration in functional monomers participates in

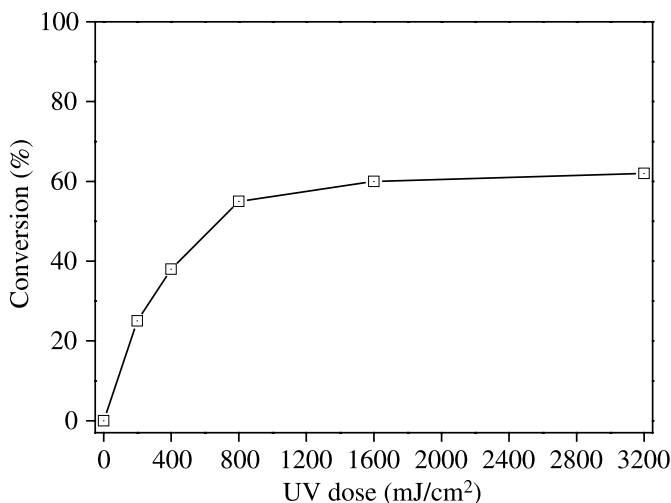


**Figure 10.** Conversion of C=C bonds at  $810\text{ cm}^{-1}$  as a function of UV dose for UV curable groups in binders blended with additional monomers.

the cross-linking reaction [32]. The FTIR spectra of UV-curable mixture composed of 2-EHA/AA/3-MTPS copolymer (2-EHA/AA/3-MTPS = 95/4.5/0.5) and DPHA and 3-MPTS (20/20 phr in binder) was determined. The conversion of C=C bond, as a function of UV dose was calculated according to the following equation:

$$\text{Conversion (\%)} = \frac{(A_{810})_0 - (A_{810})_t}{(A_{810})_0} \times 100,$$

where  $(A_{810})_0$  is the IR absorbance at  $810\text{ cm}^{-1}$  before UV irradiation;  $(A_{810})_t$  is the IR absorbance  $\text{cm}^{-1}$  after UV irradiation.

The conversion of C=C bonds in the blend increased sharply as the UV dose was increased to  $200\text{ mJ/cm}^2$  (Fig. 10). This is because the entanglement and/or orientation of multifunctional monomer around the acrylic copolymer induced a rapid radical chain reaction, resulting in increased reactivity [7]. The conversion of C=C bonds were not 100%. The remaining C=C bonds might have remained unreacted after the action of the photo-initiator because it was possible that they were trapped in the cross-linked polymer network.

### 3.4. FE-SEM Observations

Another aim of this study was to observe the morphology using FE-SEM (Fig. 11) and to investigate the contaminants of the polymers on the surface of the Si-wafers by XPS (Fig. 12). Some PSAs might remain on the Si-wafers after the releasing of the tapes. Figure 11 indicates the influence of the UV dose. In the ‘pick-up’ process, it is very important to consider whether there is PSA remaining, as the Si-wafer becomes thinner [25]. The increase of UV dose suggests more cross-linking

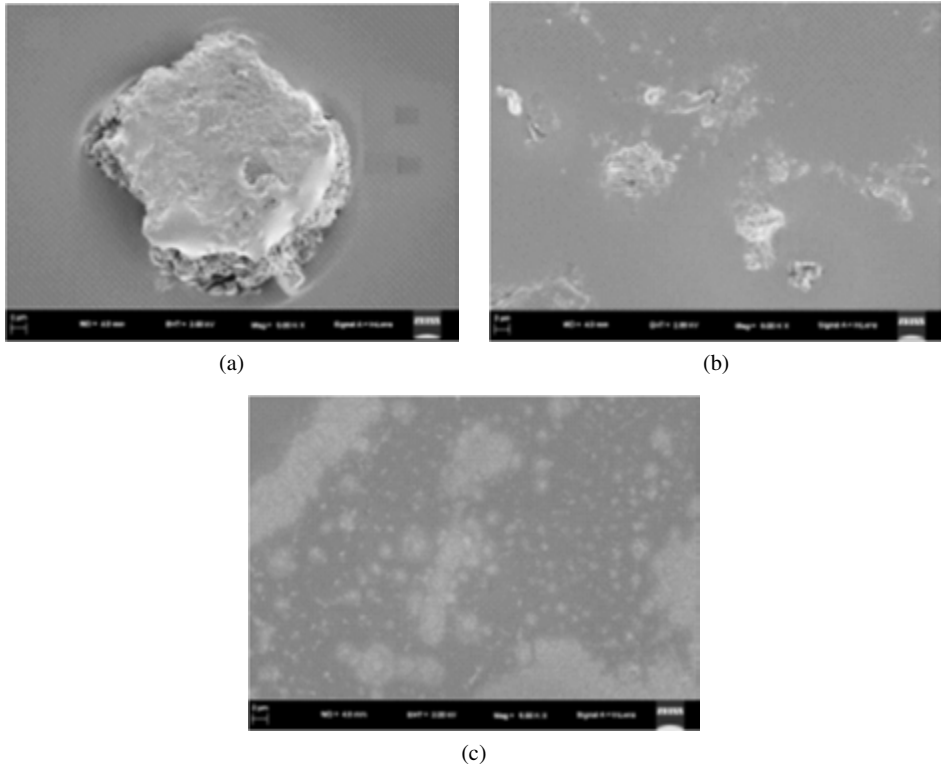


**Figure 11.** Field-emission scanning electron images of UV-cured acrylic PSAs at UV dose with  $0 \text{ mJ/cm}^2$  (a),  $800 \text{ mJ/cm}^2$  (b),  $1600 \text{ mJ/cm}^2$  (c).

reactions [33]. The efficient UV dose was found to be greater than  $1600 \text{ mJ/cm}^2$  for all the specimens.

### 3.5. XPS Analysis

Analysis by XPS was used to obtain the surface compositions of the residue on the Si-wafer after peeling at different UV doses. Figure 12 shows the  $\text{C}_{1s}$  curve-fitted core-level spectrum with one major peak of binding energy of  $284.6 \text{ eV}$  corresponding to the C–C/C–H functional groups [27, 34–36]. In addition, a peak was observed at  $283.9 \text{ eV}$  in the  $\text{C}_1$  spectra, which was assigned to an inhomogeneous charging effect on the polymer surface due to its insulating nature [37]. The above C atoms were derived from the acrylic base polymer [28]. As shown in Fig. 12, the peak at  $284.6 \text{ eV}$ , which was linked directly to the properties of the polymer (C–C and C–H), decreased with increasing UV dose. On the other hand, the  $\text{Si}_{2p}$  peaks around  $100$  and  $103 \text{ eV}$  ( $\text{SiO}_2$ ) increased with increasing UV dose. These results are in agreement with reference values [38–40]. As listed in Table 1, the amount of carbon decreased with increasing UV dose while the amount of silicon increased on the surface of the silicon wafer, as a result of the cross-linking of the acrylic PSAs.

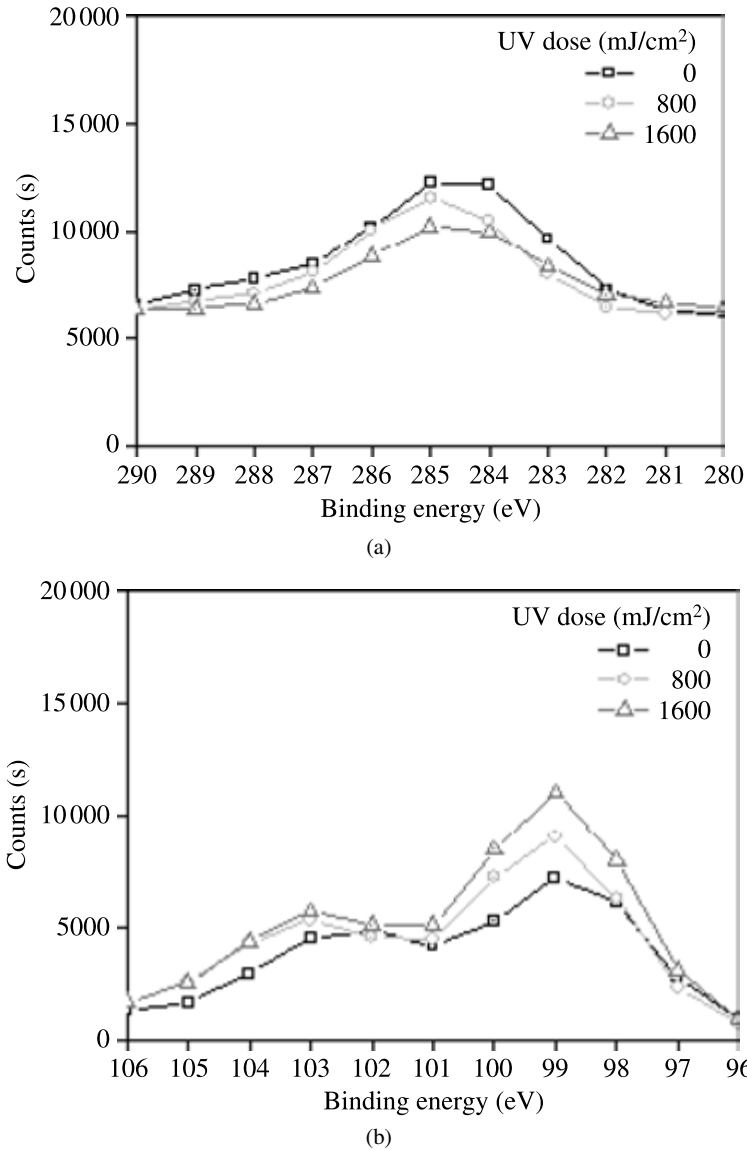


**Figure 12.**  $C_{1s}$  (a) and  $Si_{2p}$  (b) XPS spectra of Si-wafer surface after peeling at varying UV dose.

#### 4. Conclusion

When working with the silicon wafer ‘pick-up’ process, it is important to consider the conditions that apply when using PSAs. Besides the UV curing of the acrylic PSAs it is necessary to pay attention to the whole process as the silicon wafers get thinner. This study investigated the suitable condition of handling PSAs using an interpenetrated network structure.

**Table 1.**Atomic concentration (%) of C<sub>1s</sub> and Si<sub>2p</sub> determined by XPS according to the UV dose

UV dose (mJ/cm <sup>2</sup> )	C <sub>1s</sub>	Si <sub>2p</sub>
0	31.81	30.01
800	24.46	34.96
1600	17.26	42.06

In this work the effect of UV-curing on the behavior and performance of the PSAs was obtained using FTIR and a 180° peel adhesive strength test. Two kinds of different UV-irradiation were considered in these experiments. One of them, the pulsed irradiation at 100 mJ/cm<sup>2</sup>, makes the adhesion strength between adhesive layers and silicon substrates weaker than does the steady irradiation. The reason why it was investigated can be understood by considering the inhomogeneous polymer network structure which was highlighted by GPC. These results indicated that the adhesive property of PSAs depends not only on its modulus but also on the interfacial phenomena such as the local distribution of cross-linked acrylate monomer or polar segments at the interface between the adhesive layer and the silicon wafer [6]. The results from the FE-SEM and XPS studies, indicated that the required condition was little residue on the silicon wafer after releasing the PSAs film at more than the certain level of UV-dose. It was shown that under such conditions the dicing of the UV-curable tapes was successful and easily peeled and made suitable for further processing.

## References

1. D. Satas (Ed.), *Handbook of Pressure Sensitive Adhesive Technology*. Satas & Associates, Warwick, RI (1999).
2. I. Benedeck and L. J. Heymans, *Pressure-Sensitive Adhesives Technology*. Marcel Dekker Inc., New York (1997).
3. Z. Czech, *Int. J. Adhes. Adhes.* **24**, 119 (2004).
4. N. Saiki, K. Inaba, K. Kishimoto, H. Seno and K. Ebe, *Journal of Solid Mechanics and Materials Engineering* **4**, 1051 (2010).
5. K. Ebe, H. Seno and O. Yamazaki, Pressure sensitive and bonding adhesives packaging stacked integrated circuits I. Investigation on the UV/thermally dual-curable formations, *J. Adhesion Soc. Japan* **40** (7), 289–297 (2004).
6. K. Ebe, H. Seno, T. Sugino and O. Yamazaki, Pressure sensitive and bonding adhesives for packaging stacked integrated circuits II. Effects of the multi-functional acrylate component on the bonding strength to copper plate, *J. Adhesion Soc. Japan* **41** (4), 128–136 (2005).
7. K. Ebe, H. Seno and K. Horigome, *J. Appl. Polym. Sci.* **90**, 436 (2003).
8. K. Ebe and T. Sasaki, *J. Appl. Polym. Sci.* **88**, 1854 (2003).
9. K. Ebe, H. Narita, K. Taguchi and T. Saito, in: *Proceedings of the Conference on Radiation Curing Asia'88*, Tokyo, p. 250 (1998).

10. K. Ebe, H. Narita, K. Taguchi, Y. Akeda and T. Saito (to FSK Corp.), US Patent 4,756,968 (1988).
11. J. H. Koelling, *Mater. Eng.* **68**, 93 (1981).
12. R. E. Bennet and M. A. Hittner (to Minnesota Mining & Manufacturing Co.), US Patent 4,286,047 (1981).
13. H.-S. Joo, Y. J. Park, H. S. Do, H.-J. Kim, S.-Y. Song and K.-Y. Choi, *J. Adhesion Sci. Technol.* **21**, 575 (2007).
14. H. Kaczmarek and C. Decker, *J. Appl. Polym. Sci. Part B: Polym. Phys.* **43**, 3316 (2005).
15. F. Sosson, A. Chateauinois and C. Creton, *J. Polym. Sci. Part B: Polym. Phys.* **43**, 3316 (2005).
16. G. Auchter, O. Aydin, A. Zettl and D. Satas, in: *Handbook of Pressure Sensitive Adhesive Technology*, D. Satas (Ed.), pp. 444–514. Satas Associates, Warwick, RI (1999).
17. L. H. Sperling, *Interpenetrating Polymer Networks and Related Materials*. Plenum Press, New York (1981).
18. A. Dubuisson, D. Ades and M. Fontanille, Homogeneous epoxyacrylic interpenetrating polymer networks: preparation and thermal properties, *Polym. Bull.* **3**, 391–398 (1980).
19. S. Tan, D. Zhang and E. Zhou, Dynamic mechanical properties of interpenetrating polymer networks based on polyacrylates and epoxy, *Acta Polym.* **47**, 507–510 (1996).
20. A. Leistner, E. Fabrycy, J. Wagner, J. Leistner and A. Bledzki, High temperature resistant adhesives based on epoxy and bismethacrylate interpenetrating networks, *Int. Polym. Sci. Technol.* **25** (11), 96–100 (1998).
21. F. J. Hua and C. P. Hu, Interpenetrating polymer networks of epoxy resin and urethane acrylate resin. 2. Morphology and mechanical property, *Eur. Polym. J.* **36** (1), 27–33 (2000).
22. H. S. Joo, H. S. Do, Y. J. Park and H.-J. Kim, *J. Adhesion Sci. Technol.* **20**, 1573 (2006).
23. H.-S. Do, J. H. Park and H.-J. Kim, *European Polymer J.* **44**, 3871 (2008).
24. Z. Czech, *Int. J. Adhes. Adhes.* **27**, 49 (2007).
25. H. S. Kim and H.-J. Kim, *Polym. Degrad. Stab.* **93**, 1544 (2008).
26. G. Wu, S. Zeng, E. Ou, P. Yu, Y. Lu and W. Xu, *Mater. Sci. Eng. C* **30**, 1030 (2010).
27. Y. W. Song, H. S. Do, H. S. Joo, D. H. Lim, S. Kim and H.-J. Kim, *J. Adhesion Sci. Technol.* **20**, 1357 (2006).
28. J. Asahara, A. Takemura, N. Hori, H. Ono and H. Matsui, *Polymer* **45**, 4917 (2004).
29. Z. Czech, H. Loclair and M. Wesolowska, *Rev. Adv. Mater. Sci.* **14**, 141 (2007).
30. D. H. Lim, H. S. Do and H.-J. Kim, *J. Adhesion Sci. Technol.* **21**, 589 (2007).
31. J. K. Kim, W. H. Kim and D. H. Lee, *Polymer* **43**, 5005 (2002).
32. T. Scherzer, *J. Polym. Sci. Part A: Polym. Chem.* **42**, 894 (2004).
33. C. Decker, K. Zahouily, D. Decker, T. Nguyen and T. Viet, *Polymer* **42**, 7551 (2001).
34. M. C. Zhang, E. T. Kang, K. G. Neoh and K. L. Tan, *Colloids Surfaces A* **176**, 139 (2001).
35. E. Uchida, H. Iwata and Y. Ikada, *Polymer* **41**, 3609 (2001).
36. E. Uchida, Y. Uyama, H. Iwata and Y. Ikada, *J. Polym. Sci. A: Polym. Chem.* **28**, 2837 (1990).
37. S. Massey, D. Roy and A. Adnot, *Nucl. Instrum. Methods Phys. Res. B* **208**, 236 (2003).
38. S. Jin and A. Atrens, *Appl. Phys. A* **42**, 149 (1987).
39. L. T. Weng, C. Poleunis, P. Bertrand, V. Carlier, M. Sclavons, P. Franquinet and R. Legras, *J. Adhesion Sci. Technol.* **9**, 859 (1995).
40. M. Bou, J. M. Martin, Th. Le Mogne and L. Vovelle, *Appl. Surface Sci.* **47**, 149 (1991).
41. M. Amagai, H. Seno and K. Ebe, *IEEE Trans. Comp. Pkg Mfg Tech. B* **18**, 119 (1995).
42. K. Ebe and T. Kondo, *J. Adhesion Soc. Japan* **33**, 251 (1997).
43. T. Ozawa, S. Ishiwata, Y. Kano and T. Kasemura, *J. Adhesion* **72**, 1 (2000).
44. D. H. Lim, H. S. Do and H.-J. Kim, *J. Appl. Polym. Sci.* **102**, 2839 (2006).